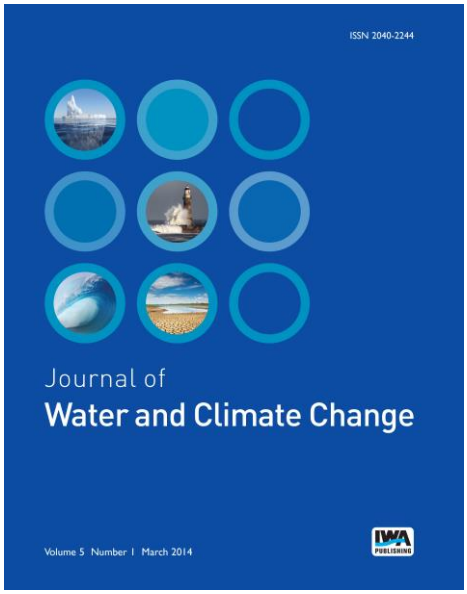

Detection and attribution of seasonal temperature changes in India with climate models in the CMIP5 archive

P. Sonali and D. Nagesh Kumar

ABSTRACT

This study analyzes the change in annual and seasonal maximum and minimum temperature (T_{max} and T_{min}) during the period 1950–2005 (i.e., second half of the 20th century). In-depth analyses have been carried out for all over India as well as for five temperature homogenous regions of India separately. First, the temporal variations of annual and seasonal T_{max} and T_{min} are analyzed, employing the trend free pre-whitening Mann-Kendall approach. Secondly, it is assessed whether the observations contain significant signals above the natural internal variability determined from a long 'piControl' experiment, using Monte Carlo simulation. Thirdly, fingerprint based formal detection and attribution analysis is used to determine the signal strengths of observed and model simulations with respect to different considered experiments. Finally, these signal strengths are compared to attribute the observed changes in T_{max} and T_{min} to different factors. All the model simulated datasets are retrieved from the CMIP5 archive. It is noticed that the emergence of observed trends is more pronounced in T_{min} compared to T_{max}. Although observed changes are not solely associated with one specific causative factor, most of the changes in T_{min} lie above the bounds of natural internal climate variability.

Key words | climate change signal, CMIP5 dataset, formal detection-attribution, natural internal climate variability, seasonal temperature, trend detection

P. Sonali
D. Nagesh Kumar (corresponding author)
Department of Civil Engineering,
Indian Institute of Science,
Bangalore 560012,
India
E-mail: *nagesh@civil.iisc.ernet.in*

P. Sonali
Divecha Centre for Climate Change,
Indian Institute of Science,
Bangalore 560012,
India

D. Nagesh Kumar
Centre for Earth Sciences,
Indian Institute of Science,
Bangalore 560012,
India

INTRODUCTION

The warming of the global climate system in the past century is unequivocal, as evidenced by a change in climate with increasing frequency, intensity, duration and spatial extension of heat waves (Åström *et al.* 2013; Estrada *et al.* 2013). Coumou *et al.* (2013) inferred the 'worldwide number of record breaking monthly temperature extremes is now on average five times larger than that expected in a climate with no long term warming'. Multiple lines of evidence show that global mean surface temperature has increased significantly during 1951 to 2010, and the enhanced greenhouse gas concentration is the most likely reason behind more than half of this observed increment and these changes are largely due to anthropogenic emissions (Intergovernmental Panel on Climate Change (IPCC) 2014). It is also virtually certain that natural internal variability alone cannot explain the observed global warming since 1951. Interpreting climate variability correctly is of paramount importance to infer its effect on humans, environment and the hydrological cycle. Human influence has been detected in major assessed components of the climate system. Solar energy, which is one of the natural external forcings, is responsible for warming the climate but its contribution is much less compared to GHGs (greenhouse gases). Moreover, the observed long-term tropospheric warming and stratospheric cooling patterns are not consistent with the expected response to solar forcing. With the support of robust evidence from various studies using different methods, assessments were made and the above statements are reported in Chapter 10 of IPCC AR5. A new generation of climate models (CMIP5), whose ability to simulate

doi: 10.2166/wcc.2015.072

historical climate has improved in many respects relative to the previous models (CMIP3), is used for these assessments shown in the AR5. Global mean surface temperature has increased by 0.74 °C ± 0.18 °C during 1906–2005 (Solomon *et al.* 2007). During the first half of the 20th century, the influence of natural internal factors in climate variation was significant as compared to the second half of the 20th century (Tol & Estrada 2013).

Two fundamental issues related to climate change, i.e., precise detection and attribution (D&A), are still challenging and need to be further addressed. Neither of these issues are simple to address. Many climate change D&A studies are available based on variables other than temperature, viz. potential evapotranspiration (Zhang *et al.* 2013a), atmospheric moisture content (Santer *et al.* 2007), rainfall (Zhang *et al.* 2007; Zhang *et al.* 2013b), extreme temperature and precipitation (Min *et al.* 2013; Zhang *et al.* 2013b; Fischer & Knutti 2014; Wuebbles *et al.* 2014), changes due to snowmelt (Pierce *et al.* 2008) and others. A number of D&A studies had been carried out at river basin and sub-basin scale in different parts of the world (Hidalgo *et al.* 2009; Jia *et al.* 2012; Mondal & Mujumdar 2012; Patterson *et al.* 2013). These studies were carried out using different methods to address the question of whether the risk of high flood events and change in stream flow can be attributed to anthropogenic climate change effect.

Natural internal variability is the chaotic variation of the climate system, which is also termed as noise in D&A analysis. Longer observed homogenous records are preferred for powerful anthropogenic signal detection from the background of natural internal variability. This demand has been met with the passing period of time. But along with the observed dataset, data of various influencing drivers from a much wider range are equally essential for climate change D&A study. The most cited method is optimal fingerprinting for climate change D&A, which was introduced by Hasselmann (1993). In the optimal fingerprint detection approach, to enhance the SNR (Signal to Noise Ratio), the climate change signal vector rotates in a direction away from the natural internal variability (Hegerl *et al.* 1996).

Research on D&A in India has been done to a lesser extent, although thorough researches have been carried out in other parts of the world (Jia *et al.* 2012; Åström *et al.* 2013; Patterson *et al.* 2013) as well as globally (Zhou *et al.* 2010; Lewis & Karoly 2013b; Ribes *et al.* 2013; Zhang *et al.* 2013b) for the last couple of decades using different methods. Miscellaneous 'event attribution' studies have also been carried out in the various regions recently (Lewis & Karoly 2013a; Shiogama *et al.* 2013; Angélil *et al.* 2014). Ribes *et al.* (2010) implemented the temporal optimal detection method for regional climate change detection. The temporal optimal detection method considers spatial information without using the spatial response pattern of internal variability. Regularized optimal fingerprinting (ROF), which is an alternative for optimal fingerprinting (which avoids the projection step), was used by Ribes *et al.* (2013) to detect and attribute the changes in the global near surface temperature. Patterson *et al.* (2013) and Xu *et al.* (2014) used 'Budyko curves' to attribute changes in stream flow due to climate and human factors.

Accelerated surface temperatures (both T_{max} and T_{min}) resulted in a change in different components of the hydrological cycle, either directly or indirectly. The open water evaporation rate has increased considerably in recent decades globally (Jung *et al.* 2010; Douville *et al.* 2013) as well as in specific parts of the world (Helfer *et al.* 2012; Huo *et al.* 2013; Liu *et al.* 2013), and is also going to change significantly in response to changes in air temperature in the future (Johnson & Sharma 2010; Zhang *et al.* 2013a). Stream flow is a significant measurable indicator of fresh water availability. There is a slight decrease in global stream flow over the second half of the 20th century (Dai *et al.* 2009). One of the cardinal descriptors influencing stream flow is temperature, and this is attested via changes in evaporation rate. T_{max} and T_{min} are among the six most commonly used variables in impact assessment studies (IPCC 2001).

The motivation of this study is primarily to overcome the following limitations noticed in the literature dealing with climate change D&A studies concerning India:

- Compared with CMIP3 (Coupled Model Inter-comparison Project phase 3), CMIP5 (Coupled Model Intercomparison Project phase 5) promoted a greater number of General Circulation Models (GCMs), which have high spatial resolution and are complex in nature (Taylor *et al.* 2012). In spite of notable improvement in models of CMIP5 over CMIP3, most of the D&A studies are mainly based on CMIP3 (Imbers *et al.* 2013; Min *et al.*

2013; Zohrabi *et al.* 2014) except for a few (Hanlon *et al.* 2013; Chen & Frauenfeld 2014). Studies based on a limited number of climate models without prior knowledge about their performance could mislead the results by adding a huge amount of uncertainties.

- Most of the detection studies have used various trend detection techniques, concentrating on a particular region. Trend detection gives the variability information over each grid point individually, whereas the formal D&A approach gives the combined information over the entire considered grid points. Although similar thorough research has been carried out for other parts of the world, there is a scarcity of climate change D&A study for India (as discussed earlier).
- A formal D&A study based on rainfall and stream flow changes over the Mahanadi river basin of India using the CMIP3 dataset has been conducted (Mondal & Mujumdar 2012), whereas our focus is on temperature using the CMIP5 dataset for all over India.
- To date, formal D&A studies either for all over India or for any temperature homogenous regions of India are not available.
- In India, there are more studies related to climate change based on rainfall as the variable of interest than studies based on temperature as the variable of interest (Sonali & Nagesh Kumar 2013).
- A study performed to analyze the spatial and temporal variability of annual, monthly, and seasonal T_{max} and T_{min} over all India and over temperature homogeneous regions in three time slots, 1901–2003, 1948–2003 and 1970–2003 by Sonali & Nagesh Kumar (2013), established a foundation for further climate change D&A study for India.

Thus from the above discussion it is realized that there is an urgent need for various D&A studies based on different combinations of parameters (space, time, variables of interest and methodologies) over India. It has been attempted to achieve this goal by detecting and attributing the changes in the seasonal T_{max} and T_{min} observed record.

This study employs formal D&A analysis (Hidalgo *et al.* 2009) to extract the inscrutable details about observed climate behavior. It primarily analyzes the cause of temperature change in the second half of the 20th century over all India and over the temperature homogeneous regions of India. The time span considered here is 1950–2005, which consists of 56 years. It may not be the second half of the 20th century exactly, but it is referred to as the same (second half of the 20th century) in this study.

This paper primarily addresses the following issues:

- How the seasonal observed T_{max} and T_{min} have changed with time.
- Whether the natural internal climate variability simulated by climate model could explain the observed variability.
- Whether it is possible to attribute the recent change in T_{max} and T_{min} to anthropogenic effects.

Initially the seasonal and annual temporal variability of T_{max} and T_{min} during the second half of the 20th century over all the regions considered (the spatial average of all the grids inside a region) are analyzed, employing the trend free pre-whitening Mann-Kendall approach.

'piControl' experiment outputs of GCM are used as a proxy for natural internal variability in the absence of long observed records. This raises the second issue of this study, whether natural internal climate variability, as simulated by the climate models, could explain the observed variability in temperature.

Finally, fingerprint based D&A analysis is used to compare the observed and model temperature signal strengths, and then attributes the observed changes in seasonal T_{max} and T_{min} to different factors including natural internal or external climate variability and climate change induced due to anthropogenic emissions.

In the following section, the details about the study area and observed and model data used are presented. Secondly, the methodology implemented is explained. Thirdly, the detailed steps followed in this study are described.

STUDY AREA AND DATASETS

Study area

The proposed formal D&A analysis mainly focuses on the surface air temperature of all over India for the period 1950 to 2005. India is divided into seven temperature homogenous regions, that is, East Coast (EC), West Coast (WC), Interior

Peninsula (IP), Northwest (NW), Northeast (NE), North Central (NC) and Western Himalaya (WH), as defined by the Indian Institute of Tropical Meteorology (source: http://www.tropmet.res.in). A graphical representation of the spatial extent of these regions is shown in Figure 1. Out of the seven regions, five regions are considered (for reasons described later) in this study in addition to all over India. Divisions of seasons are based on conventional meteorological seasons: January-February (winter), March–May (pre monsoon), June-September (monsoon) and October-December (post monsoon). Focused parameters are seasonal and annual T_{max} and T_{min}, which constitutes ten detection variables (or temperature indices) namely Annual T_{max}, Annual T_{min}, JF T_{max}, JF T_{min}, MAM T_{max}, MAM T_{min}, JJAS T_{max}, JJAS T_{min}, OND T_{max} and OND T_{min}. These are the ten detection variables used for this present formal D&A analysis. Any changes in climate could be directly detected by analyzing temperature, and it has a significant influence on all the components of the hydrologic cycle. Detection variables and temperature indices are interchangeably used in this study.

Observed dataset

The gridded observed T_{max} and T_{min} dataset at $1^\circ \times 1^\circ$ resolutions for the period 1969–2009 is obtained from the India Meteorological Department (IMD) (Srivastava *et al.* 2009).

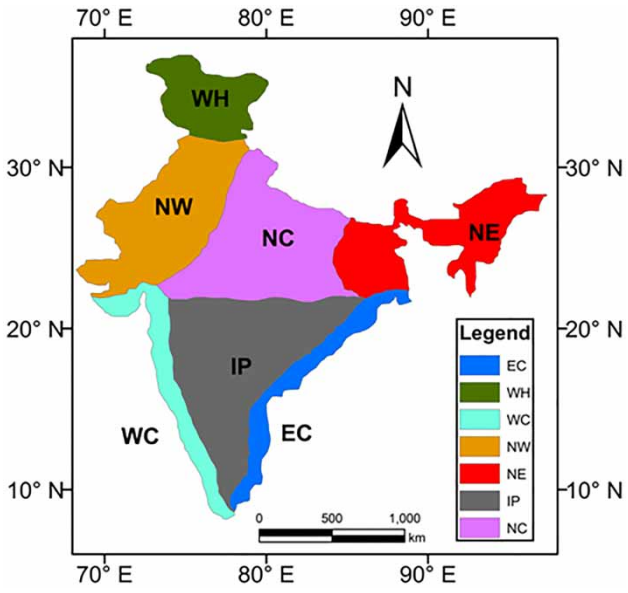

Figure 1 | Seven temperature homogenous regions of India.

These 41 years of observed data do not cover the entire second half of the 20th century. All the climate experiments used for the attribution study have used data up to 2005. As the present study focuses on the second half of the 20th century (1950–2005), the latest version CRU3.21 dataset (http://badc.nerc.ac.uk/browse/badc/cru/data/cru_ts/cru_ts_3.21), which provides observed monthly T_{max} and T_{min} for the period 1901 to 2012 at a resolution of $0.5^\circ \times 0.5^\circ$, is considered as a proxy for the observed dataset after comparing with the IMD dataset. The CRU3.21 data were interpolated to IMD grid points, and absolute gridded average differences were obtained for the common period (1969–2005). This practice was followed at annual, seasonal (JF, MAM, JJAS, OND) and monthly scales for both T_{max} and T_{min}. Consistently better correlation is ascertained (between CRU3.21 and IMD temperature datasets) at all the grid points except a few ($>30^\circ$ North and $>88^\circ$ East) in all the considered cases. Most of the poorly correlated grid points were located in the Western Himalaya region and partially in the Northeast region. Hence, these two regions are excluded from this study.

Model dataset

For D&A analysis, climate model simulations are essential along with observations. D&A analysis is sensitive to bias and uncertainty present in the model simulations. By considering high skill climate models, bias and uncertainty can be reduced to the greatest possible extent. Sonali *et al.* (2015) carried out a climate model assessment study. They found that there is a significant improvement in CMIP5 as compared to CMIP3 models, both at monthly and seasonal scale. They concluded that all the models, irrespective of generations, have better skill in simulating T_{min} compared to T_{max}. These conclusions (Sonali *et al.* 2015) were the motivation to consider models separately for T_{max} and T_{min} from CMIP5.

Based on the aforementioned model evaluation study and the availability of considered experiments, nine models each for T_{max} and T_{min} were chosen for this study. The five sets of experiments, that is, 'piControl', 'historical', 'historicalMisc', 'historicalGHG' and 'historicalNat', are used in this D&A analysis.

The 'piControl' experiment is the approximation of the natural climate system, and it is the long-term generated model simulation. It explains only natural internal variability due to the usage of a fixed GHG level from pre-industrial times (the year 1850). The 'historical' experiments are forced by best estimates of historical natural forcings (solar, volcanic) and anthropogenic emissions (well mixed GHGs, aerosols and ozone). Both 'historical' and 'piControl' experiments are available for all CMIP5 models.

The 'historicalMisc' experiment consists of historical simulations, but with other individual forcing agents or a combination of forcings. It is less realistic than the 'historical' experiment. 'HistoricalMisc' simulations provide information about the relative importance of different forcings during the historical period (http://cmip-pcmdi.llnl.gov/cmip5/docs/historical_Misc_forcing.pdf). 'historicalGHG' is a historical simulation but with greenhouse gas forcing only. Likewise 'historicalNat' is historical simulation with natural external forcing only. The difference between 'historical' and 'historicalGHG' experiments is the inclusion of aerosols in 'historical'. These three experiments possess data for the same period as the 'historical' experiment (Taylor *et al.* 2012) but are not available for all climate models. The terms 'experiment' and 'scenario' are used interchangeably in this study.

Outputs of different experiments from 18 CMIP5 climate models for T_{max} and T_{min} during the second half of the 20th century have been used in this analysis. Since most of the considered GCMs have multiple realizations, the ensemble of realizations associated with a particular GCM is considered as the representative value for that GCM.

In this study, formal D&A analysis is carried out by considering ten detection variables for all over India as well as for five temperature homogenous regions of India separately. Analysis for all over India was done on $2.5^\circ \times 2.5^\circ$ interpolated grid points, whereas individual regional analysis was done on $1.5^\circ \times 1.5^\circ$ grid points. All the observed and modeled datasets were interpolated using the nearest neighbor interpolation technique. A few studies in the literature, at global and sub-global scale data, are re-gridded to a coarser resolution (for example $5^\circ \times 5^\circ$) for smoothing and to reduce the effect of noise (Zhang *et al.* 2007; Hanlon *et al.* 2013; Lewis & Karoly 2013b). $2.5^\circ \times 2.5^\circ$interpolation shows that in all the five regions, grid points are fewer in number whereas $1.5^\circ \times 1.5^\circ$grids had more. Due to this difference, the study for all over India was based on $2.5^\circ \times 2.5^\circ$, while the study for individual regions was based on $1.5^\circ \times 1.5^\circ$. After interpolation to the two scales (1.5° and 2.5°), the values were compared with the original data. It was found that the differences were negligible between the interpolated and original data.

METHODOLOGY

Fingerprint based formal D&A approach

The formal D&A approach based on fingerprinting of climate change relates the climate responses to model responses. This has some advantages compared to the two extreme ways of trying to detect a significant variable change using a mean value or by searching in the full variable space (Jia *et al.* 2012). The general idea for fingerprint based D&A is to reduce the problem of multiple dimensions to a low dimension problem (Hegerl *et al.* 1996; Santer *et al.* 2007). The fingerprint is the expected pattern of climate response to anthropogenic forcing, and it is searched for in the observed and model responses. Formal D&A analysis primarily requires three components, that is, anthropogenic ensemble (from the 'historic' experiment) to calculate the fingerprint, long control simulation (from the 'piControl' experiment) for measuring the statistical significance of the result, and observational data, which is projected onto the fingerprint.

In the optimal fingerprint detection, the optimization process requires a prior estimation of noise associated with the fingerprint to enhance the signal to noise ratio. Due to the unavailability of noise based observation, part of a control simulation is used for optimization, which is not allowed to be a part of the detection process to satisfy independent assumption. Results show that there is little difference between optimized and non-optimized versions (Santer *et al.* 2007; Hidalgo *et al.* 2009; Hanlon *et al.* 2013). Additionally, non-optimized analysis includes the whole of the control simulations for detection. Hence, the non-optimized version of formal D&A is used.

The intent of this approach is to obtain the signature or fingerprint of variable change in the low dimensional space. The fingerprint is the leading Empirical Orthogonal Function (EOF) of anthro ensemble mean seasonal anomalies

obtained from the 'historical' experiment. Suppose a matrix '*A*' in which the x-axis (column) represents space and the y-axis (row) represents time (a row is a map at a particular time), then the co-variance matrix of *A* is used further to identify the fingerprint which is the leading EOF and explains the maximum variability. This fingerprint is further used to find the signal strength (also known as the attribution index) corresponding to observation and different model experiments. Signal strength '*S*' is the trend of projected data onto the fingerprint.

$$S = \text{trend}\ (f(x).T(x, t)) \tag{1}$$

where $f(x)$ is the fingerprint and $T(x,t)$ is the time series of either observation or the model. Here (Equation (1)) the trend is the slope of the least square best fit line. Similarly, uncertainty in the signal strength is calculated from Monte Carlo simulation. Comparison between observed and model signal strengths corresponding to different experiments is helpful to attribute the observed changes to a specific causative factor.

Averaging over multiple realizations reduces the noise and enhances the signals. Uncertainty due to each model's systematic error cancels out by considering the multi-model mean, resulting in the reduction of uncertainty in the attribution study. Reduced uncertainty helps in splitting up the signal properly at global or sub-global scale. The data at each grid are expressed in anomaly form, and the anomaly is calculated with respect to the climatological mean calculated over the considered period, i.e., 1950–2005. All the models are weighted equally for multi-model ensemble average calculation. Ensemble average (i.e., multi-model mean, MMM) and use of leading EOF are the ways to reduce noise. The anthro ensemble mean anomalies (obtained from the 'historical' experiment) are used to identify the fingerprint. Signal strengths for each model and multi-model mean are obtained for all the considered experiments except the 'piControl' experiment. Each climate model's outputs for the 'piControl' experiment are of unequal length. In the case of the 'piControl' experiment, data from all considered climate models are added together, which results in 6,276 and 4,590 years for T_{max} and T_{min} respectively.

An exhaustive characterization of natural internal variability is essential in D&A analysis to justify the statement 'anthropogenic emissions are the *very likely* cause of climate change' (IPCC 2007; Imbers *et al.* 2013). It is of utmost importance to obtain the probability of observed signal strengths that lie outside the bounds of the control signal strength distribution. Following Hidalgo *et al.* (2009), Monte Carlo simulations are used to derive the likelihood estimation of the observed signal strength traced in the distribution of signal strength obtained from the 'piControl' experiment. A group of *p*-members (of length *n*) was randomly selected from the available control independent run (from the 'piControl' experiment) segments. Here *p* is the number of ensemble members ($p = 9$ for 'historical', $p = 3$ for the other three, i.e., 'historicalMisc', 'historical GHG' and 'historicalNat' experiments for the detection variables related to T_{max}). Here $n =$ the length of observed record, i.e., 56 years. From the group of randomly selected *p*-members, ensemble average signal strength was calculated, and this procedure was repeated 10,000 times to derive the distribution of control signal strength. This control signal strength distribution is obtained for individual as well as a combination of all considered climate models. Then it is checked how likely it is that the observed signal strength would be picked up from the control signal strength distribution. These results are shown in Table 1, Table 2 and Table 3 respectively for different cases (cases are explained in 'Results and discussion').

Trend free pre-whitening (TFPW) with Mann-Kendall (MK) test (Yue *et al.* 2002)

The rank based non parametric Mann-Kendall (Mann 1945; Kendall 1975) test is used for trend detection. The Mann-Kendall test statistic S_{MK} is defined by

$$S_{\text{MK}} = \sum_{i=2}^{n} \sum_{j=1}^{i-1} \text{sign}\ (x_i - x_j) \tag{2}$$

where *n* is the length of the data series x_i and x_j are the sequential data in the series and

$$\text{sign}(x_i - x_j) = \begin{cases} -1 & \text{for} \quad (x_i - x_j) < 0 \\ 0 & \text{for} \quad (x_i - x_j) = 0 \\ 1 & \text{for} \quad (x_i - x_j) > 0 \end{cases} \tag{3}$$

Table 1 | Results from the signal strength comparison to determine whether the observed signal strengths are statistically different from the signal strength distribution obtained from model 'piControl' experiment for All_India and EC_India

Model [All_India_T_{max}] piControl Experiment	Annual T_{max}	JF T_{max}	MAM T_{max}	JJAS T_{max}	OND T_{max}	Model [All_India_T_{min}] piControl Experiment	Annual T_{min}	JF T_{min}	MAM T_{min}	JJAS T_{min}	OND T_{min}
BNU-ESM	×	×	×	×		ACCESS1.3	×	×	O	O	O
Combined all Models (T_{max})	×	×	×	×	O	Combined all Models (T_{min})	O	O	O	O	O
CCSM4	×	×	×	×	×	CCSM4	×	×	O	O	×
CESM1-BGC	×	×	×	×	O	CESM1-BGC	O	O	×	O	O
CNRM-CM5	×	×	×	×	×	GFDL-ESM2G	×	×	O	O	×
MIROC5	×	×	×	×	×	MIROC5	O	O	O	O	O
MPI-ESM LR	×	×	×	×	O	MRI-CGCM3	×	×	O	O	O
MPI-ESM P	×	×	×	×	×	NOR-ESM1 M	O	O	O	O	O
Model [EC_India_T_{max}] piControl Experiment	**Annual T_{max}**	**JF T_{max}**	**MAM T_{max}**	**JJAS T_{max}**	**OND T_{max}**	**Model [EC_India_T_{min}] piControl Experiment**	**Annual T_{min}**	**JF T_{min}**	**MAM T_{min}**	**JJAS T_{min}**	**OND T_{min}**
BNU-ESM	×	×	×	×	O	ACCESS1.3	×	O	O	O	×
Combined all Models (T_{max})	×	×	×	×	O	Combined all Models (T_{min})	O	O	O	O	O
CCSM4	×	×	×	×	O	CCSM4	O	O	O	O	×
CESM1-BGC	×	×	×	×	O	CESM1-BGC	O	O	O	O	O
CNRM-CM5	×	×	×	×	O	GFDL-ESM2G	×	×	O	O	×
MIROC5	×	×	×	×	O	MIROC5	O	O	O	O	O
MPI-ESM LR	×	×	×	×	O	MRI-CGCM3	×	×	O	O	×
MPI-ESM P	×	×	×	×	O	NOR-ESM1 M	O	O	O	O	O

$$E[S_{\mathrm{MK}}] = 0 \tag{4}$$

$$\mathrm{Var}(S_{\mathrm{MK}}) = \frac{n(n-1)(2n+5) - \sum_{k-1}^{q} t_k(t_k-1)(2t_k+5)}{18} \tag{5}$$

where t_k is the number of ties for the k^{th} value and q is the number of tied values. In variance formula, the second part of the numerator is for tied censored data. The standardized test statistic Z_{MK} is defined as

$$Z_{\mathrm{MK}} = \begin{cases} \dfrac{S_{\mathrm{MK}} - 1}{\sqrt{\mathrm{Var}\,(S_{MK})}} & \text{if} \quad S_{\mathrm{MK}} > 0 \\ 0 & \text{if} \quad S_{\mathrm{MK}} = 0 \\ \dfrac{S_{\mathrm{MK}} + 1}{\sqrt{\mathrm{Var}\,(S_{\mathrm{MK}})}} & \text{if} \quad S_{\mathrm{MK}} < 0 \end{cases} \tag{6}$$

To test the monotonic trend at α significance level, the null hypothesis of no trend is rejected if the absolute value of the standardized test statistic Z_{MK} is greater than $Z_{MK1-\alpha/2}$ obtained from the standard normal cumulative distribution tables. The effect of serial correlation is taken care of by the trend free pre-whitening approach explained in the following paragraph.

First find the magnitude of the slope using the Sen's slope (SS) (Sen 1968) approach for the considered time series. Then assuming the AR(1) process, de-trend the linear trend from the time series. If the lag-1 correlation coefficient of the de-trended time series is significant at a defined level, then apply the MK test to the de-trended pre-whitened series recombined with the estimated slope (using the SS approach), else apply the MK test to the original series. In summary, the methodology for the present analysis is depicted in a flow chart (Figure 2).

Table 2 | Results from the signal strength comparison to determine whether the observed signal strengths are statistically different from the signal strength distribution obtained from model 'piControl' experiment for WC_India and IP_India

Model [WC_India_T_{max}] piControl Experiment	Annual T_{max}	JF T_{max}	MAM T_{max}	JJAS T_{max}	OND T_{max}	Model [WC_India_T_{min}] piControl Experiment	Annual T_{min}	JF T_{min}	MAM T_{min}	JJAS T_{min}	OND T_{min}
BNU-ESM	×	×	×	×	×	ACCESS1.3	×	×	×	O	×
Combined all Models (T_{max})	×	×	×	×	O	Combined all Models (T_{min})	×	×	×	O	×
CCSM4	×	×	×	×	O	CCSM4	×	×	×	O	×
CESM1-BGC	×	×	×	×	O	CESM1-BGC	×	×	×	O	×
CNRM-CM5	×	×	×	×	×	GFDL-ESM2G	×	×	×	O	×
MIROC5	×	×	×	×	O	MIROC5	×	×	×	O	×
MPI-ESM LR	×	×	×	×	×	MRI-CGCM3	×	×	×	O	×
MPI-ESM P	×	×	×	×	×	NOR-ESM1 M	×	×	×	O	×
Model [IP_India_T_{max}] piControl Experiment	**Annual T_{max}**	**JF T_{max}**	**MAM T_{max}**	**JJAS T_{max}**	**OND T_{max}**	**Model [IP_India_T_{min}] piControl Experiment**	**Annual T_{min}**	**JF T_{min}**	**MAM T_{min}**	**JJAS T_{min}**	**OND T_{min}**
BNU-ESM	×	×	×	×	×	ACCESS1.3	×	×	O	O	×
Combined all Models (T_{max})	×	×	×	×	O	Combined all Models (T_{min})	×	×	O	O	×
CCSM4	×	×	×	×	O	CCSM4	×	×	O	O	×
CESM1-BGC	×	×	×	×	O	CESM1-BGC	×	×	×	O	×
CNRM-CM5	×	×	×	×	×	GFDL-ESM2G	×	×	O	O	×
MIROC5	×	×	×	×	×	MIROC5	×	×	O	O	×
MPI-ESM LR	×	×	O	×	O	MRI-CGCM3	×	×	O	×	×
MPI-ESM P	×	×	×	×	×	NOR-ESM1 M	×	×	×	O	×

RESULTS AND DISCUSSION

In this study the variations of T_{max} and T_{min} during four seasons, that is, winter (JF), pre monsoon (MAM), monsoon (JJAS) and post monsoon (OND), and at annual level, are examined by applying the TFPW-MK trend detection technique. The observed time series of ten detection variables (defined earlier) for each considered region (i.e., five temperature homogenous regions and all over India (displayed in Figure 1)) are obtained by spatially averaging over all the grids in that region. Further temporal variability during the second half of the 20th century (i.e., 1950–2005) is analyzed using the TFPW-MK approach. The TFPW-MK test statistic is evaluated at 5% significance level. A significant upward trend in T_{max} is observed during the post monsoon in most of the considered regions, whereas an upward trend in T_{min} is detected in most of the seasons for all over India and the EC region. The total number of significant trends in T_{min} is greater compared to T_{max}. These findings agree with the previous inferences available in the literature to a large extent (Kothawale & Rupa Kumar 2005; Sonali & Nagesh Kumar 2013).

Uncertainty arises due to spatially averaging in the case of trend detection analysis. Results and conclusions obtained from this analysis may serve as a primary exemplum. The formal D&A approach has the advantage of considering space and time together in calculating maximum variability (leading EOF) which results in the reduction of noise (already explained in the methodology section).

Formal D&A analysis is carried out to assess the change in seasonal temperature of India over the period 1950–2005. Results reported here are for all over India as well as for the temperature homogenous regions of India, considering ten detection variables. Signal strengths and

Table 3 | Results from the signal strength comparison to determine whether the observed signal strengths are statistically different from the signal strength distribution obtained from model 'piControl' experiment for NW_India and NC_India

Model [NW_India_T_{max}] piControl Experiment	Annual T_{max}	JF T_{max}	MAM T_{max}	JJAS T_{max}	OND T_{max}	Model [NW_India_T_{min}] piControl Experiment	Annual T_{min}	JF T_{min}	MAM T_{min}	JJAS T_{min}	OND T_{min}
BNU-ESM	×	×	×	×	×	ACCESS1.3	O	×	O	×	×
Combined all Models(T_{max})	×	×	×	×	×	Combined all Models(T_{min})	O	O	O	O	O
CCSM4	×	×	×	×	×	CCSM4	×	×	×	O	×
CESM1-BGC	×	×	×	×	×	CESM1-BGC	O	O	×	O	×
CNRM-CM5	×	×	×	×	×	GFDL-ESM2G	O	×	×	×	×
MIROC5	×	×	×	×	×	MIROC5	O	O	O	O	O
MPI-ESM LR	×	×	×	O	×	MRI-CGCM3	O	×	×	O	O
MPI-ESM P	×	×	×	×	×	NOR-ESM1 M	O	O	×	×	×
Model [NC_India_T_{max}] piControl Experiment	**Annual T_{max}**	**JF T_{max}**	**MAM T_{max}**	**JJAS T_{max}**	**OND T_{max}**	**Model [NC_India_T_{min}] piControl Experiment**	**Annual T_{min}**	**JF T_{min}**	**MAM T_{min}**	**JJAS T_{min}**	**OND T_{min}**
BNU-ESM	×	×	O	×	×	ACCESS1.3	×	×	O	×	×
Combined all Models(T_{max})	O	×	O	×	×	Combined all Models(T_{min})	O	×	O	O	O
CCSM4	×	×	×	×	×	CCSM4	×	×	×	O	×
CESM1-BGC	O	×	O	×	×	CESM1-BGC	×	×	×	×	×
CNRM-CM5	O	×	O	×	×	GFDL-ESM2G	×	×	×	×	×
MIROC5	×	×	×	×	×	MIROC5	O	×	O	O	O
MPI-ESM LR	×	×	O	×	×	MRI-CGCM3	×	×	O	×	O
MPI-ESM P	×	×	O	×	×	NOR-ESM1 M	×	×	×	×	O

corresponding 95% confidence intervals are obtained for observed as well as for model data with respect to different experiments. Individual and multi-model means corresponding to different experiments are compared with the observations.

Before this comparison, Monte Carlo simulation was used to estimate the likelihood of observations drawn from the control run distribution. Details of this are already mentioned in the methodology section. Results are shown for all ten detection variables over different regions in Table 1 (all over India, EC), Table 2 (WC, IP) and Table 3 (NW, NC) respectively. In these Tables, a cross ('×') indicates the observed signal strength drawn from the control run ('piControl' experiment) distribution at 5% significance level and a circle ('O') indicates the opposite. These analyses are carried out individually for models having control run data ('piControl' experiment) for more than 500 years. Seven models for T_{max} (excluding CESM1-CAM5 and CESM1_FASTCHEM) and seven models for T_{min} (excluding MIROC4 h and CESM1-CAM5) are considered for this analysis. The same analysis is again performed by combining all the nine models together, results are shown in the same tables (Tables 1–3). Considering six regions and five seasons, 30 cases are constructed for T_{max} and 30 for T_{min}. For each case there are eight options (seven individual models and one combination of all the nine models). It is considered that if the likelihood estimation analysis shows that the observed signal strength is different from the control run distribution in more than two options, including the combination of all the models, it is different. For natural internal climate variability assessment, long control run simulations are suitable. Thus the combined model control run distribution is statistically significant to a greater extent compared to the individual models. Assuming

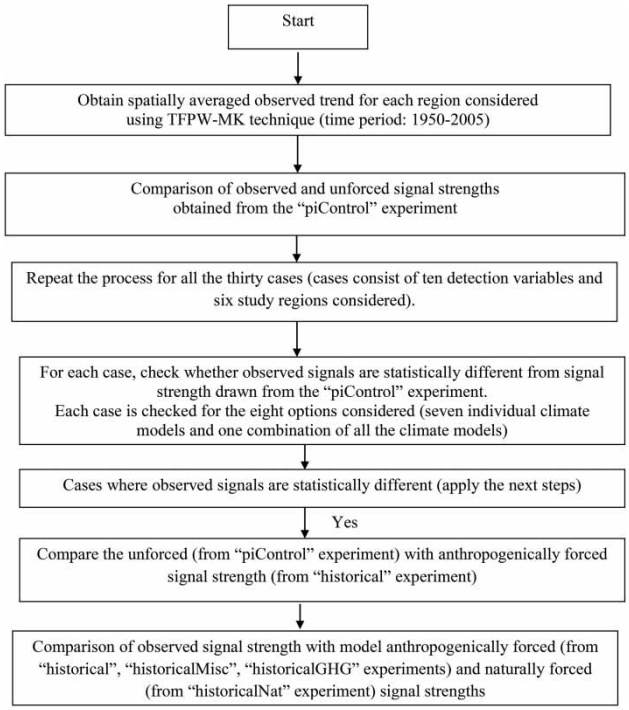

Figure 2 | Flow chart for fingerprint based formal D&A approach.

estimated natural internal climate variability based on the model (from the 'piControl' experiment) is reliable, it is noticed that 6 out of 30 cases for T_{max} and 22 for T_{min} are different from the natural internal climate variability at the 5% significance level. No previous results exist to support or contradict our findings.

In summary, these results indicate that the observed T_{min} indicators (annual and seasonal) over most of the regions are different from the natural internal climate variability. Twenty-eight out of 60 cases (discussed earlier) are reported in Table 4. Thus the above 28 cases are considered for the multi-model mean (MMM) 'historical' experiment. The results are shown in Table 5 and Table 6 for T_{max} and T_{min} respectively. For all the six cases of T_{max} (mentioned in Table 4), the results are consistent with observation (Table 5). This implies the signal strengths corresponding to observation and multi-model mean 'historical' experiments are simultaneously different from the control run distribution. Whereas in T_{min}, five out of 22 cases are inconsistent (highlighted in Table 6). The discrepancies in climate

Table 4 | Cases where the test is passed (i.e., observed signal strengths are statistically different from the signal strength distribution obtained from model 'piControl' experiment). This '†' sign indicates where the test is passed

Region	Annual T_{max}	JF T_{max}	MAM T_{max}	JJAS T_{max}	OND T_{max}	Annual T_{min}	JF T_{min}	MAM T_{min}	JJAS T_{min}	OND T_{min}
All_India					†	†	†	†	†	†
EC_India					†	†	†	†	†	†
WC_India					†				†	
IP_India					†			†	†	
NW_India						†	†	†	†	†
NC_India	†		†			†		†	†	†

Table 5 | Results from the signal strength comparison to determine whether the MMM 'historical' signal strengths are statistically different from the signal strength distribution obtained from the model 'piControl' experiment (cases related to T_{max})

Model [All_India_T_{max}] piControl Experiment	Annual T_{max} NC_India	MAM T_{max} NC_India	OND T_{max} All_India	OND T_{max} EC_India	OND T_{max} WC_India	OND T_{max} IP_India
BNU-ESM	×	O	×	O	O	×
Combined all Models (T_{max})	O	O	O	O	O	O
CCSM4	×	×	×	O	O	O
CESM1-BGC	O	O	O	O	O	O
CNRM-CM5	O	O	×	×	×	×
MIROC5	×	×	×	×	O	×
MPI-ESM LR	O	O	O	×	×	×
MPI-ESM P	O	O	×	×	×	×

Table 6 | Results from the signal strength comparison to determine whether the MMM 'historical' signal strengths are statistically different from the signal strength distribution obtained from the model 'piControl' experiment (cases related to T_{min})

Model [All_India_T_{min}] piControl Experiment	Annual T_{min} All_India	Annual T_{min} EC_India	Annual T_{min} NW_India	Annual T_{min} NC_India	JF T_{min} All_India	JF T_{min} EC_India	JF T_{min} NW_India	MAM T_{min} All_India	MAM T_{min} EC_India	MAM T_{min} IP_India	MAM T_{min} NW_India
ACCESS1.3	×	×	×	×	×	×	×	×	O	×	×
Combined all Models (T_{min})	O	O	O	×	O	O	O	O	O	O	×
CCSM4	×	×	×	×	×	×	×	×	×	×	×
CESM1-BGC	×	×	O	×	O	×	O	×	×	×	×
GFDL-ESM2G	×	×	×	×	×	×	×	×	O	×	×
MIROC5	O	O	O	×	O	O	×	O	O	O	×
MRI-CGCM3	×	×	×	×	×	×	×	×	×	O	×
NOR-ESM1 M	×	×	×	×	×	O	×	×	O	×	×

Model [All_India_T_{min}] piControl Experiment	MAM T_{min} NC_India	JJAS T_{min} All_India	JJAS T_{min} EC_India	JJAS T_{min} WC_India	JJAS T_{min} IP_India	JJAS T_{min} NW_India	JJAS T_{min} NC_India	OND T_{min} All_India	OND T_{min} EC_India	OND T_{min} NW_India	OND T_{min} NC_India
ACCESS1.3	×	O	O	O	O	O	×	×	×	×	×
Combined all Models (T_{min})	×	O	O	O	O	O	O	O	O	×	×
CCSM4	×	O	O	O	O	O	O	×	×	×	×
CESM1-BGC	×	O	O	O	O	O	O	×	O	×	×
GFDL-ESM2G	×	O	O	O	O	×	×	×	×	×	×
MIROC5	×	O	O	O	O	O	O	O	O	×	×
MRI-CGCM3	×	O	×	O	×	O	×	O	×	×	×
NOR-ESM1 M	×	O	O	O	O	O	×	O	×	×	×

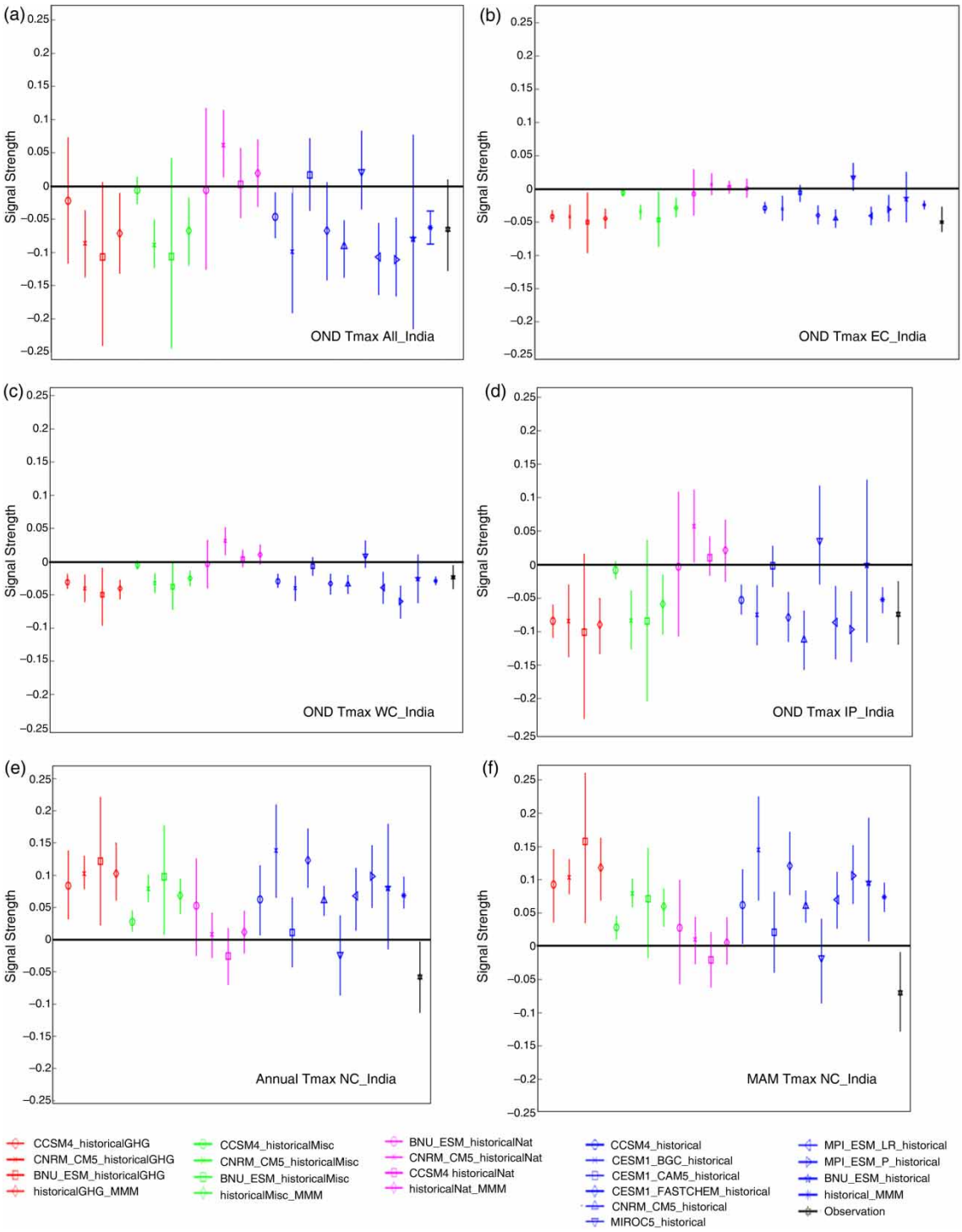

Figure 3 | Signal strengths along with 95% confidence interval for all considered models individually and MMM of models with respect to different experiments shown for all the highlighted cases in Table 4 related to T_{max}.

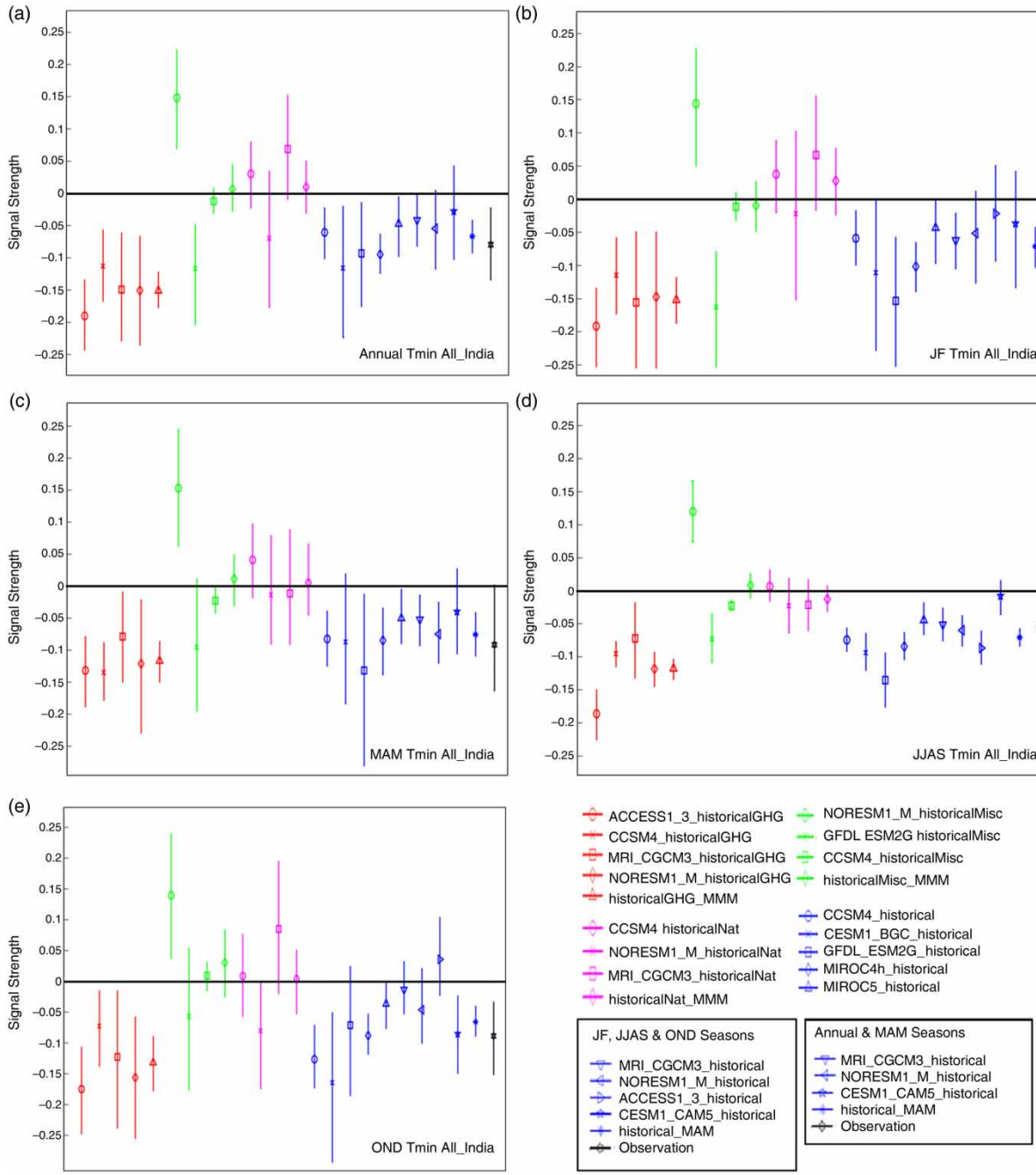

Figure 4 | Signal strengths along with 95% confidence interval for all considered models individually and MMM of models with respect to different experiments shown for all the highlighted cases in Table 4 related to T_{min} of all over India.

model output for T_{max} and T_{min} may be due to improper simulation of the cloud radiation process (Zhou *et al.* 2010).

For the cases reported in Table 4, the value of signals, including the 95% confidence interval (CI) for observation, are obtained and compared with the signal strength corresponding to different model experiments, that is, 'historicalGHG', 'historicalMisc', 'historicalNat' and 'historical'. Results are obtained for individual models as well as for multi-model means (stated as historicalGHG_MMM, historicalMisc_MMM, historicalNat_MMM, and historical_MMM in the legends of

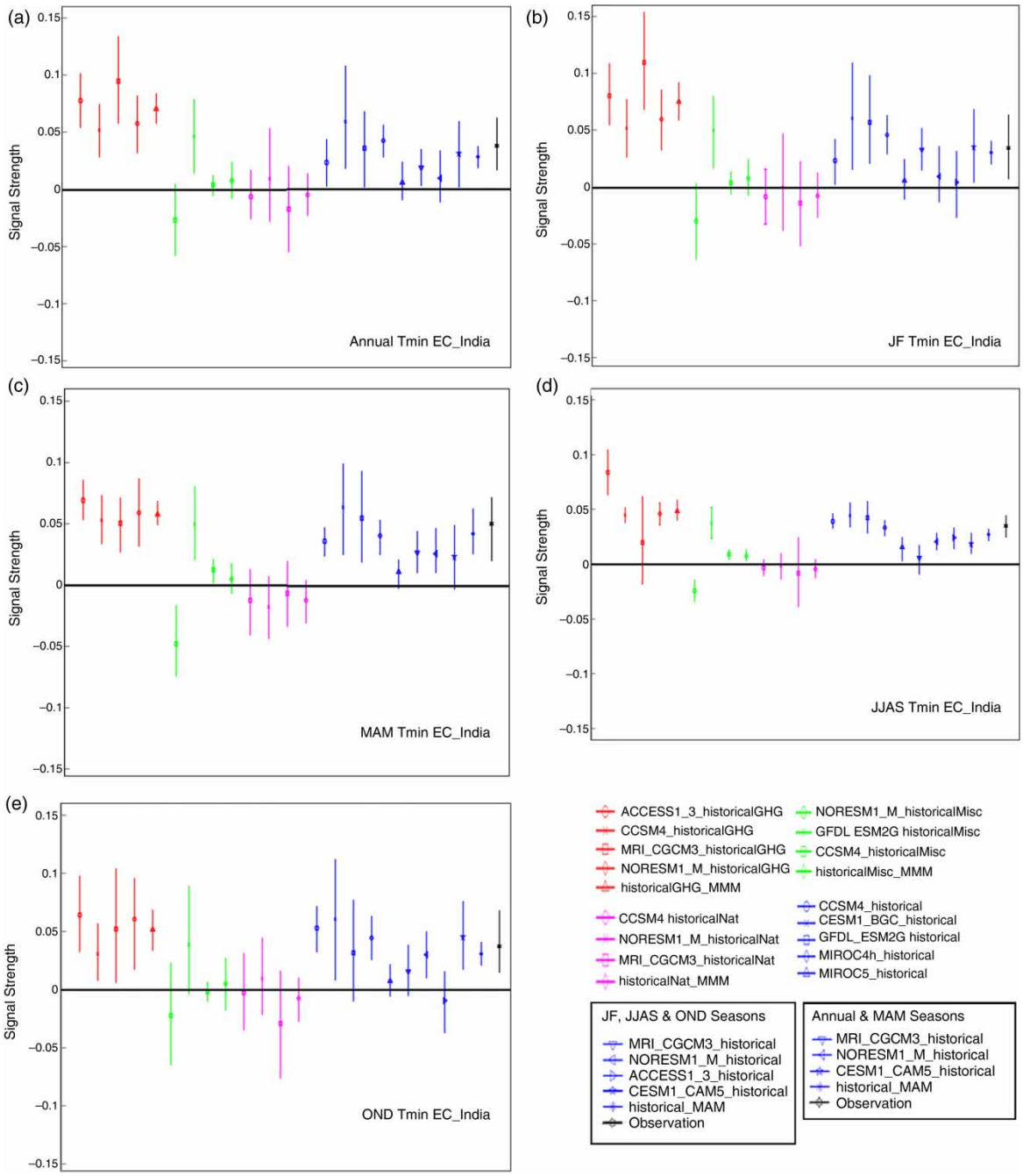

Figure 5 | Signal strengths along with the 95% confidence interval for all considered models individually and MMM of models with respect to different experiments shown for all the highlighted cases in Table 4 related to T_{min} of EC India.

Figures 3–8) with respect to different experiments and shown in Figures 3–8 ['historicalGHG' (red), 'historicalMisc' (green), 'historicalNat' (magenta), 'historical' (blue) and observations (black); please refer to the online version of this paper to see these figures in colour]. It is observed that historical T_{min} simulations (from the 'historical' experiment) in the ACCESS1.3 model deviates significantly from the multi-model mean during pre-monsoon season (MAM), which in turn affects Annual T_{min} (as Annual T_{min} is the minimum temperature among all the months). This model's historical

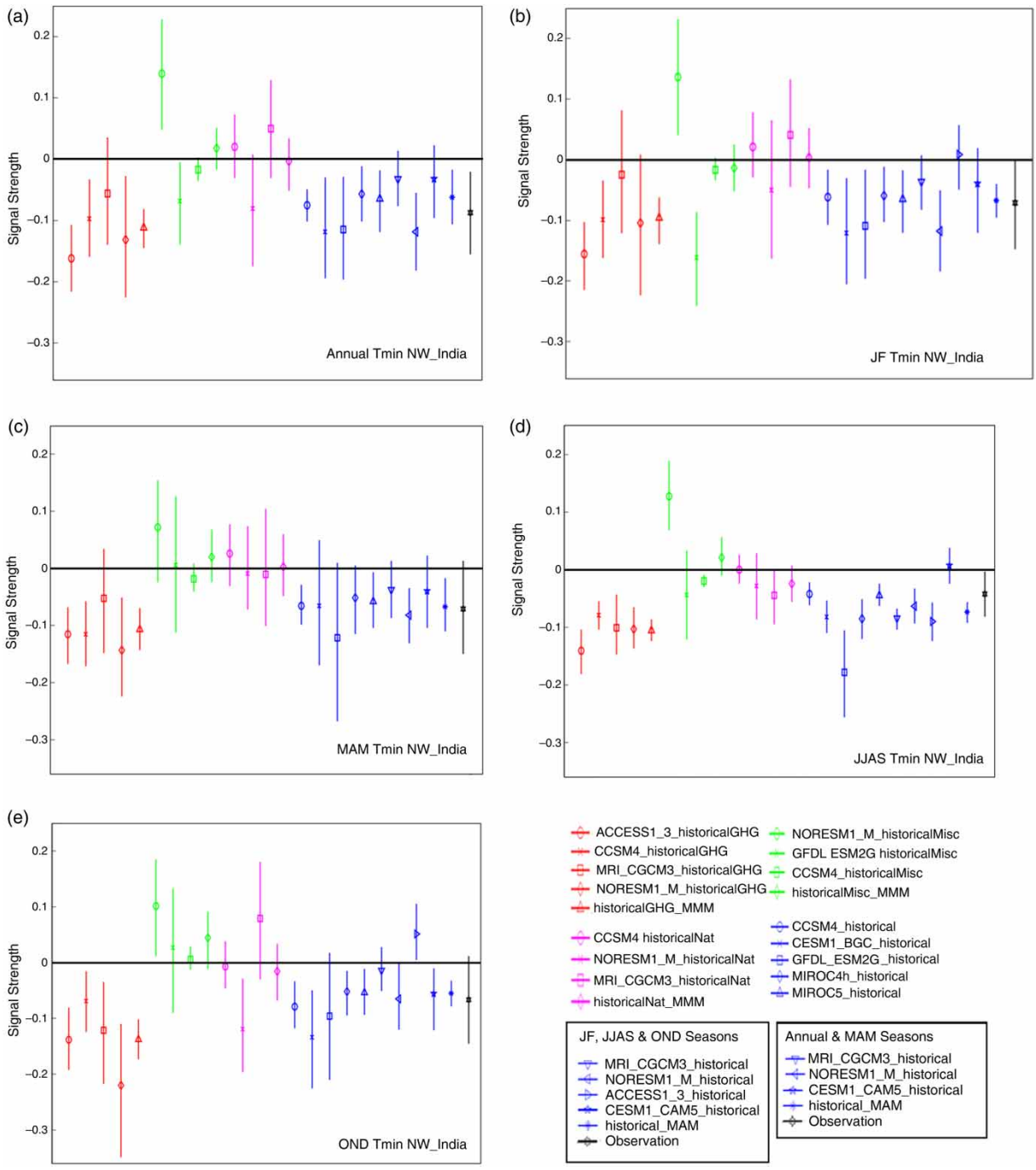

Figure 6 | Signal strengths along with the 95% confidence interval for all considered models individually and MMM of models with respect to different experiments shown for all the highlighted cases in Table 4 related to T_{min} of NW India.

simulation output during these seasons (Annual T_{min} and MAM T_{min}) is highly variable (high variance) as compared to other models. This kind of behavior in the ACCESS1.3 model is not observed in other experiments and seasons. The difference in the multi-model mean with and without considering the ACCESS1.3 model, checked using Wilcoxon signed-rank, is statistically significant. Hence the ACCESS1.3 model is not used for Annual T_{min} and MAM T_{min}. In Figures 4–8,

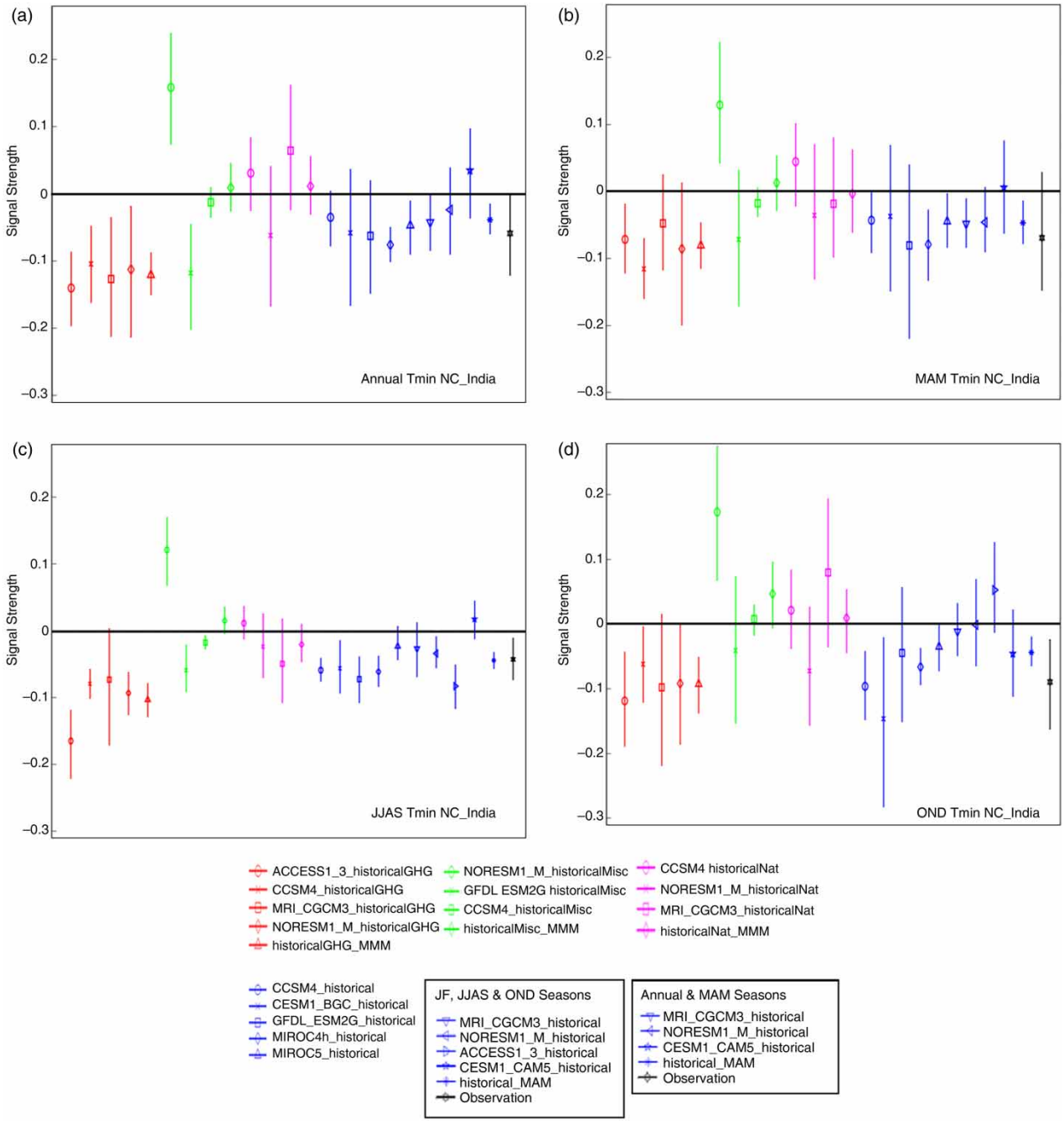

Figure 7 | Signal strengths along with the 95% confidence interval for all considered models individually and MMM of models with respect to different experiments shown for all the highlighted cases in Table 4 related to T_{min} of NC India.

legends are different for these two seasons (Annual, MAM), i.e., excluding model ACCESS1.3 (for the 'historical' experiment).

Figure 3 represents the cases corresponding to T_{max}. Figures 4–6 represent cases corresponding to T_{min} in all over India, EC and NW respectively. In these three regions, observed signal strengths of T_{min} indices corresponding to all the seasons (Annual T_{min}, JF T_{min}, MAM T_{min}, JJAS T_{min} and OND T_{min}) are significantly different from the control run signal strength distribution. Results corresponding to the NC

region are reported in Figure 7. Due to the lower number of cases corresponding to IP and WC regions (observations significantly different from control distribution; Table 4), these results are shown together in Figure 8. In most of the cases the multi-model mean signal strength of 'historical' and 'historicalGHG' experiments matches with observed signal strength, for example: OND T_{max} all over India, JF T_{min} all over India, JF T_{min} EC India, OND T_{min} EC India, JF T_{min} NW India, MAM T_{min} NW India etc. Except for 2 cases (Annual T_{max} NC India; MAM T_{max} NC India) out of 28, MMM signal strengths of the 'historical' experiment have the same sign as the observed signal strength. In some cases, the signal strength of the MMM 'historicalNat' experiment either possesses the opposite sign to the observed signal strength or is relatively close to zero.

For unequivocal attribution of observed changes, these should be consistent with the expected pattern from any anthropogenic forcing ('historical' or 'historicalGHG', 'historicalMisc') and inconsistent with natural forcing ('historicalNat') model simulations simultaneously. In the present study, unequivocal attribution is not possible as shown in Figures 3–8.

In the present study, there may be scope for uncertainties due to the equal weights assigned to each model for multi-model mean calculation and due to the ignorance of land use change information. It is noticed that the performance of the climate model in simulating Indian temperature is season dependent. Although unequivocal attribution was not possible, it is confirmed that most of the observed seasonal changes in India (due to T_{min}) over the period 1950–2005 are outside the range expected because of natural internal climate variability.

CONCLUSION

Climate change creates a driving force for the hydrological cycle. Thus better understanding of changes in climate is

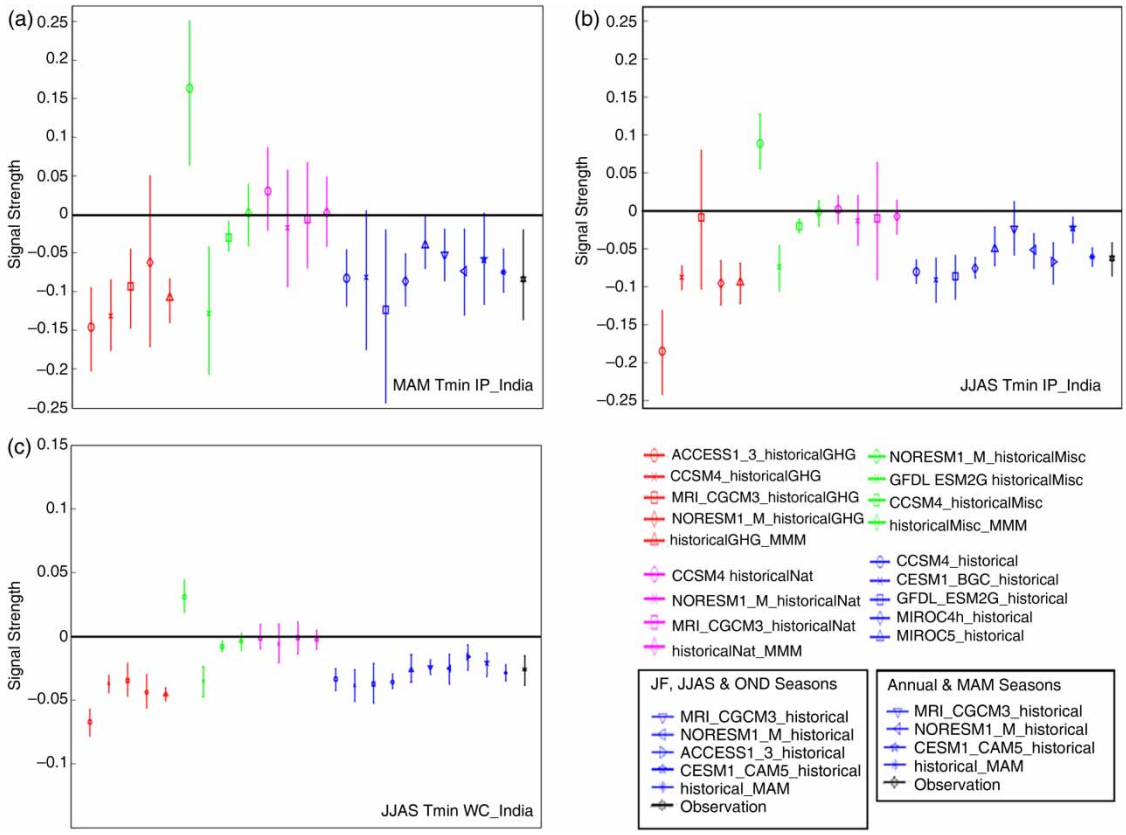

Figure 8 | Signal strengths along with the 95% confidence interval for all considered models individually and MMM of models with respect to different experiments shown for all the highlighted cases in Table 4 related to T_{min} of IP India & WC India.

essential for water resources management. In the past, most of the decisions related to water supply planning and management were based on a stationary climate, which does not hold good presently due to human induced effects.

In the recent past, variations in surface temperature have been significant both at continental and global level at daily and monthly time steps. Due to this, a notable number of studies have shown interest in this analysis. Rigorous D&A analyses had been performed recently to differentiate whether the recent changes happened due to natural internal climate variability or due to human induced effects.

In this pursuit, the current study examines the variation of T_{max} and T_{min} over India during the second half of the 20th century. The main aim of this study is to assess the extent to which the GCMs can simulate the observed major variability and trends. Further D&A studies could be carried out to deduce future climate change information and uncertainty. Performing D&A studies on a wider range of spatial and temporal scales (different seasons) will provide a full view of recent changes in climate. It is concluded that the natural internal variability of the climate system of India might not be the major cause of changes in most of the cases related to T_{min}.

ACKNOWLEDGEMENT

This work is partly supported by the Ministry of Earth Sciences, Government of India (MOES/ATMOS/PP-IX/09). We acknowledge the assistance of the World Climate Research Programme's Working Group on Coupled Modeling, which is responsible for CMIP, and we thank the climate modeling groups for producing and making available their model outputs. For CMIP, the US Department of Energy's Program for Climate Model Diagnosis and Intercomparison provided coordinating support and led to the development of software infrastructure in partnership with the Global Organization for Earth System Science Portals. We also thank the IMD for the gridded temperature dataset.

REFERENCES

Angélil, O., Stone, D. A., Tadross, M., Tummon, F., Wehner, M. & Knutti, R. 2014 Attribution of extreme weather to anthropogenic greenhouse gas emissions: sensitivity to spatial and temporal scales. *Geophys. Res. Lett.* **41** (6), 2150–2155.

Åström, D. O., Forsberg, B., Ebi, K. L. & Rocklöv, J. 2013 Attributing mortality from extreme temperatures to climate change in Stockholm, Sweden. *Nat. Clim. Chang.* **3** (12), 1050–1054.

Chen, L. & Frauenfeld, O. W. 2014 Surface air temperature changes over the 20th and 21st centuries in China simulated by 20 CMIP5 models. *J. Clim.* **27**, 3920–3937.

Coumou, D., Robinson, A. & Rahmstorf, S. 2013 Global increase in record-breaking monthly-mean temperatures. *Clim. Chang.* **118** (3–4), 771–782.

Dai, A., Qian, T., Trenberth, K. E. & Milliman, J. D. 2009 Changes in continental fresh water discharge from 1948 to 2004. *J. Clim.* **22** (10), 2773–2792.

Douville, H., Ribes, A., Decharme, B., Alkama, R. & Sheffield, J. 2013 Anthropogenic influence on multi-decadal changes in reconstructed global evapotranspiration. *Nat. Clim. Chang.* **3** (1), 59–62.

Estrada, F., Perron, P. & Martínez-López, B. 2013 Statistically derived contributions of diverse human influences to twentieth-century temperature changes. *Nat. Geosci.* **6**, 1050–1055.

Fischer, E. M. & Knutti, R. 2014 Detection of spatially aggregated changes in temperature and precipitation extremes. *Geophys. Res. Lett.* **41**, 547–554.

Hanlon, H. M., Morak, S. & Hegerl, G. C. 2013 Detection and prediction of mean and extreme European summer temperatures with a multimodel ensemble. *J. Geophys. Res. Atmos.* **118**, 9631–9641.

Hasselmann, K. 1993 Optimal fingerprints for the detection of time-dependent climate change. *J. Clim.* **6** (10), 1957–1971.

Hegerl, G. C., Von Storch, H., Hasselmann, K., Santer, B. D., Cubasch, U. & Jones, P. D. 1996 Detecting greenhouse-gas-induced climate change with an optimal fingerprint method. *J. Clim.* **9** (10), 2281–2306.

Helfer, F., Lemckert, C. & Zhang, H. 2012 Impacts of climate change on temperature and evaporation from a large reservoir in Australia. *J. Hydrol.* **475**, 365–378.

Hidalgo, H. G., Das, T., Dettinger, M. D., Cayan, D. R., Pierce, D. W., Barnett, T. P., Bala, G., Mirin, A., Wood, A. W., Bonfils, C., Santer, B. D. & Nozawa, T. 2009 Detection and attribution of streamflow timing changes to climate change in the Western United States. *J. Clim.* **22** (13), 3838–3855.

Huo, Z., Dai, X., Feng, S., Kang, S. & Huang, G. 2013 Effect of climate change on reference evapotranspiration and aridity index in arid region of China. *J. Hydrol.* **492**, 24–34.

Imbers, J., Lopez, A., Huntingford, C. & Allen, M. 2013 Sensitivity of climate change detection and attribution to the characterization of internal climate variability. *J. Clim.* **27**, 3477–3491.

IPCC 2001 *The scientific basis: third assessment report of the Intergovernmental Panel on Climate Change*. Cambridge University Press, Cambridge, UK.

IPCC 2007 *The physical science basis: fourth assessment report of the Intergovernmental Panel on Climate Change*. Cambridge University Press, Cambridge, UK.

IPCC 2014 *Climate Change 2013: The Physical Science Basis: Working Group I Contribution to the IPCC Fifth Assessment Report*. Cambridge University Press, Cambridge, UK.

Jia, Y., Ding, X., Wang, H., Zhou, Z., Qiu, Y. & Niu, C. 2012 Attribution of water resources evolution in the highly water-stressed Hai River Basin of China. *Water Resour. Res.* **48** (2), W02513.

Johnson, F. & Sharma, A. 2010 A comparison of Australian open water body evaporation trends for current and future climates estimated from class A evaporation pans and general circulation models. *J. Hydrometeorol.* **11** (1), 105–121.

Jung, M., Reichstein, M., Ciais, P., Seneviratne, S. I., Sheffield, J., Goulden, M. L., Bonan, G., Cescatti, A., Chen, J., De Jeu, R., Dolman, A. J., Eugster, W., Gerten, D., Gianelle, D., Gobron, N., Heinke, J., Kimball, J., Law, B. E., Montagnani, L., Mu, Q., Mueller, B., Oleson, K., Papale, D., Richardson, A. D., Roupsard, O., Running, S., Tomelleri, E., Viovy, N., Weber, U., Williams, C., Wood, E., Zaehle, S. & Zhang, K. 2010 Recent decline in the global land evapotranspiration trend due to limited moisture supply. *Nature* **467** (7318), 951–954.

Kendall, M. G. 1975 *Rank Correlation Methods*. Charles Griffin, London.

Kothawale, D. R. & Rupa Kumar, K. 2005 On the recent changes in surface temperature trends over India. *Geophys. Res. Lett.* **32** (18), L18714.

Lewis, S. C. & Karoly, D. J. 2013a Anthropogenic contributions to Australia's record summer temperatures of 2013. *Geophys. Res. Lett.* **40** (14), 3705–3709.

Lewis, S. C. & Karoly, D. J. 2013b Evaluation of historical diurnal temperature range trends in CMIP5 models. *J. Clim.* **26** (22), 9077–9089.

Liu, M., Tian, H., Yang, Q., Yang, J., Song, X., Lohrenz, S. E. & Cai, W. J. 2013 Long-term trends in evapotranspiration and runoff over the drainage basins of the Gulf of Mexico during 1901–2008. *Water Resour. Res.* **49** (4), 1988–2012.

Mann, H. B. 1945 Nonparametric tests against trend. *Econometrica* **13**, 245–259.

Min, S. K., Zhang, X., Zwiers, F., Shiogama, H., Tung, Y. S. & Wehner, M. 2013 Multi-model detection and attribution of extreme temperature changes. *J. Clim.* **26** (19), 7430–7451.

Mondal, A. & Mujumdar, P. P. 2012 On the basin scale detection and attribution of human induced climate change in monsoon precipitation and streamflow. *Water Resour. Res.* **48** (10), W10520.

Patterson, L. A., Lutz, B. & Doyle, M. W. 2013 Climate and direct human contributions to changes in mean annual streamflow in the South Atlantic, USA. *Water Resour. Res.* **49** (11), 7278–7291.

Pierce, D. W., Barnett, T. P., Hidalgo, H. G., Das, T., Bonfils, C., Santer, B. D., Bala, G., Dettinger, M. D., Cayan, D. R., Mirin, A., Wood, A. W. & Nozawa, T. 2008 Attribution of declining western US snowpack to human effects. *J. Clim.* **21** (23), 6425–6444.

Ribes, A., Azaïs, J. M. & Planton, S. 2010 A method for regional climate change detection using smooth temporal patterns. *Clim. Dyn.* **35** (2–3), 391–406.

Ribes, A., Planton, S. & Terray, L. 2013 Application of regularised optimal fingerprinting to attribution. Part I: method, properties and idealised analysis. *Clim. Dyn.* **41** (11–12), 2817–2836.

Santer, B. D., Mears, C., Wentz, F. J., Taylor, K. E., Gleckler, P. J., Wigley, T. M. L., Barnett, T. P., Boyle, J. S., Brüggemann, W., Gillett, N. P., Klein, S. A., Meehl, G. A., Nozawa, T., Pierce, D. W., Stott, P. A., Washington, W. M. & Wehner, M. F. 2007 Identification of human-induced changes in atmospheric moisture content. *PNAS* **104** (39), 15248–15253.

Sen, P. K. 1968 Estimates of the regression coefficient based on Kendall's tau. *J. Am. Statist. Assoc.* **63** (324), 1379–1389.

Shiogama, H., Watanabe, M., Imada, Y., Mori, M., Ishii, M. & Kimoto, M. 2013 An event attribution of the 2010 drought in the South Amazon region using the MIROC5 model. *Atmos. Sci. Lett.* **14** (3), 170–175.

Solomon, S., Qin, D., Manning, M., Chen, Z., Marquis, M., Averyt, K. B., Tignor, M. & Miller, H. L. 2007 *Climate Change 2007: The Physical Science Basis: Working Group I Contribution to the Fourth Assessment Report of the IPCC* (Vol. 4). Cambridge University Press, Cambridge, UK.

Sonali, P. & Nagesh Kumar, D. 2013 Review of trend detection methods and their application to detect temperature changes in India. *J. Hydrol.* **476**, 212–227.

Sonali, P., Nagesh Kumar, D. & Nanjundiah, R. S. 2015 Intercomparison of CMIP5 and CMIP3 simulations of the 20th century maximum and minimum temperatures over India and detection of climatic trends. *Theor. Appl. Climatol.* (under review).

Srivastava, A. K., Rajeevan, M. & Kshirsagar, S. R. 2009 Development of a high resolution daily gridded temperature data set (1969–2005) for the Indian region. *Atmos. Sci. Lett.* **10** (4), 249–254.

Taylor, K. E., Stouffer, R. J. & Meehl, G. A. 2012 An overview of CMIP5 and the experiment design. *Bull. Am. Meteorol. Soc.* **93** (4), 485–498.

Tol, R. S. & Estrada, F. 2013 Estimating the global impacts of climate variability and change during the 20th century. Working Paper Series 6213, Department of Economics, University of Sussex.

Wuebbles, D., Meehl, G., Hayhoe, K., Karl, T. R., Kunkel, K., Santer, B., Wehner, M., Colle, B., Fischer, E. M., Fu, R., Goodman, A., Janssen, E., Lee, H., Li, W., Long, L. N., Olsen, S., Sheffield, J. & Sun, L. 2014 CMIP5 Climate model analyses: climate extremes in the United States. *Bull. Am. Meteorol. Soc.* **95**, 571–583.

Xu, X., Yang, D., Yang, H. & Lei, H. 2014 Attribution analysis based on the Budyko hypothesis for detecting the dominant cause of runoff decline in Haihe basin. *J. Hydrol.* **510**, 530–540.

Yue, S., Pilon, P., Phinney, B. & Cavadias, G. 2002 The influence of autocorrelation on the ability to detect trend in hydrological series. *Hydrol. Process.* **16** (9), 1807–1829.

Zhang, X., Zwiers, F. W., Hegerl, G. C., Lambert, F. H., Gillett, N. P., Solomon, S., Stott, P. A. & Nozawa, T. 2007 Detection of human influence on twentieth-century precipitation trends. *Nature* **448** (7152), 461–465.

Zhang, D., Liu, X. & Hong, H. 2013a Assessing the effect of climate change on reference evapotranspiration in China. *Stoch. Environ. Res. Risk Assess.* **27** (8), 1871–1881.

Zhang, X., Wan, H., Zwiers, F. W., Hegerl, G. C. & Min, S. K. 2013b Attributing intensification of precipitation extremes to human influence. *Geophys. Res. Lett.* **40** (19), 5252–5257.

Zhou, L., Dickinson, R. E., Dai, A. & Dirmeyer, P. 2010 Detection and attribution of anthropogenic forcing to diurnal temperature range changes from 1950 to 1999: Comparing multi-model simulations with observations. *Clim. Dyn.* **35** (7–8), 1289–1307.

Zohrabi, N., Massah Bavani, A., Goodarzi, E. & Eslamian, S. 2014 Attribution of temperature and precipitation changes to greenhouse gases in northwest Iran. *Quat. Int.* **345**, 130–137.

First received 12 May 2015; accepted in revised form 11 September 2015. Available online 13 October 2015